A GENERALISED METHOD FOR RATCHET ANALYSIS OF STRUCTURES UNDERGOING ARBITRARY THERMO-MECHANICAL LOAD HISTORIES

M. Lytwyn[a], H.F. Chen[a*] and A.R.S. Ponter[b]

[a]*Department of Mechanical & Aerospace Engineering,*
University of Strathclyde, Glasgow, G1 1XJ, UK

[b]*Department of Engineering,*
University of Leicester, Leicester, LE1 7RH, UK

Abstract

A novel approach is presented based upon the Linear Matching Method framework in order to directly calculate the ratchet limit of structures subjected to *arbitrary* thermo-mechanical load histories. Traditionally, ratchet analysis methods have been based upon the fundamental premise of decomposing the cyclic load history into cyclic and constant components respectively, in order to assess the magnitude of additional constant loading a structure may accommodate before ratcheting occurs. The method proposed in this paper, for the first time, accurately and efficiently calculates the ratchet limit with respect to a proportional variation between the cyclic primary *and* secondary loads, as opposed to an additional primary load only. The method is a strain based approach and utilises a novel convergence scheme in order to calculate an approximate ratchet boundary based upon a predefined target magnitude of ratchet strain per cycle. The ratcheting failure mechanism evaluated by the method leads to less conservative ratchet boundaries compared to the traditional Bree solution. The method yields the total and plastic strain ranges as well as the ratchet strains for various levels of loading between the ratchet and limit load boundaries. Two example problems have been utilised in order to verify the proposed methodology.

Keywords: *Linear Matching Method (LMM), Shakedown, Ratchet, Cyclic Plasticity, Direct Methods*

[*]*Corresponding author. mailto:* haofeng.chen@strath.ac.uk

1. Introduction

Power plant components in engineering environments which are subjected to thermo-mechanical load histories are often susceptible to the various failure phenomena associated with cyclic plasticity. In common nuclear structural integrity codes such as ASME III Subsection NB-3222.5 [1] and ASME III Subsection NH Appendix T, paragraph T-1332(c) [2], structures are assessed against the potential for ratcheting to occur through the derivations provided by the seminal works of Miller [3] and Bree [4]; which entailed a thin cylinder subjected to a cyclic secondary thermal gradient in tandem with a primary steady state mechanical load, using an elastic perfectly plastic (EPP) material basis. The work of Bree [4] was based on the significant assumption that a constant pressure component remained across the vessel upon reactor shutdown (with the thermal loading being completely removed). More realistic practical scenarios may actually involve simultaneous increases in thermal and mechanical loading, such as the increase in pressure and temperature of steam in a pipe or pressure vessel. Early work investigating alternative loading sequences for the generation of load interaction plots can be seen by Ng & Moreton [5-7]. The primary emphasis of this work was to analyse the ratchet limit of the Bree cylinder when both the cyclic secondary load varied as well as the cyclic primary load, both in terms of out-of-phase and in-phase variations between the cyclic thermal and mechanical loads. Reinhardt [8] has elaborated on the effects that these load variations have upon the ratchet limit with respect to the ASME III Code, whilst Abdel-Karim [9] has investigated in-phase thermo-mechanical loadings on an axially restrained tube under variable internal pressure and temperature (as commonly found in the LISA publications of Staat & Heitzer [10]. Bradford [11] has recently presented an analytical solution for the modified Bree problem; with a primary membrane stress cycling in-phase with a secondary bending stress, complete with comprehensive definitions of the relevant plastic and ratchet strains per cycle as well as the revised Bree failure assessment diagram.

The Bree problem essentially represents a one dimensional plane stress problem and allows for five cyclic plasticity responses to become evident under various combinations of loading, namely; purely elastic cycling, strict shakedown (elastic shakedown), global shakedown (alternating or reversed plasticity), ratcheting or plastic collapse. These responses can be represented in terms of cyclic plastic strain evolution; whereby an initial transient phase is followed a steady cycle period; in which the failure response of each mechanism may be characterised using either Fig. 1, which depicts the relevant plastic strain evolution of each failure response, or a typical load-interaction (Bree) diagram. As is evident in Fig. 1, *strict shakedown* is

typified by the cessation of any plastic straining per load cycle followed by the return of elastic cycling; *global shakedown* represents a closed loop hysteresis during the steady cycle period in which plastic straining occurs within each load cycle but with no net increment of plastic strain; *ratcheting* involves a net strain increment of plastic strain per load cycle (which is of constant magnitude per cycle under EPP conditions) with a failure mechanism eventually arising after a limited number of load cycles; which is attributed to the accumulation of the net plastic strain increments.

In order to assess these various cyclic failure mechanisms using modern finite element software, standard incremental calculations may be used, typically for verification purposes, as such methods possess the ability to analyse any type of load cycle. However these methods are often computationally expensive (especially for complex 3D models) and the results can often vary due to user interpretation and experience.

Direct Cyclic Analysis (DCA) [12] is a prominent numerical method which is capable of assessing the steady cyclic response of a structure, as it is based on a Fourier series methodology which calculates the structural response (based on the displacement) of a problem regardless of any load combinations, but with the inherent computational expense of requiring the full load cycle to be analysed. Recent developments have utilised DCA in tandem with an automated search algorithm that involves a significant number of trial and error calculations and eventually yields the ratchet limit [13], as applied in Rolls-Royce's Hierarchical Finite Element Framework (HFEF) [14].

Several other direct computational methods have been developed in order to assess the steady cyclic state and ratchet limit of structures, including the Linear Matching Method (LMM) [15-20], the lower bound Non-Cyclic Method [21 & 22], the Hybrid Procedure [23] (which is another constituent method of Rolls-Royce's HFEF [14]) and the residual stress decomposition method (RSDM) [24]; which seeks to decompose the residual stresses in the steady cycle period for a predefined magnitude of cyclic loading. The recently published RSDM-S method [25] utilises the RSDM in order to evaluate the shakedown limits of structures undergoing undefined magnitudes of cyclic loading. A recently published variation of the Hybrid method [23] has been implemented in the form of a lower bound ratchet analysis method by Jappy et al [26, 27].

Other numerical methods relevant for ratchet analysis include the isotropic Uniform Modified Yield method (UMY) and anisotropic Load Dependent Yield Modification method (LDMY) of

Abou-Hanna and McGreevy [28] (which have both emerged from the work of Gokhfeld's simplified ratchet method [29]) and the non-linear superposition method of Muscat et al [30, 31]. Abdalla has also recently presented a methodology similar to the basis of the non-linear superposition method in the form of a simplified method which has also seen development with respect to hardening models beyond perfect plasticity [32, 33].

The LMM is a *direct* analysis method which seeks to model the behaviour of a structure under the action of cyclic loads via repetitive linear simulations involving a matching modulus; which is used to replicate the actual nonlinear plastic response of a problem both spatially and in time. The LMM was derived on the basis of Koiter's upper bound formulation [34], with the Refs [15, 16] illustrating convergence of the LMM upper bounds for the first time with respect to shakedown and plastic collapse limits, with the novel numerical development presented in this paper the latest phase in the development of the LMM. The initial development of the LMM for ratchet analysis involved a two stage method devised by Ponter and Chen [17-19], which was capable of assessing two load points in the defined load cycle, before subsequently being extended to include multiple load points in [20]. Recently, the two stage LMM procedure for ratchet analysis has been expanded upon via the addition of a novel lower bound approach by Ure et al [35].

Similar to other direct ratchet analysis methods [e.g. 21-23, 26, 27], the existing LMM framework for ratchet analysis [17-20] is restricted to providing solutions in lieu of the original premise of the classic Bree problem; whereby a constant (primary) load component is added to a predefined cyclic load history in order to ascertain the ratchet limit. The main reasoning behind doing so stems from splitting the assessment of the residual stress history into separate constant and varying residual components respectively.

An initial numerical attempt at analysing the modified thermo-mechanical histories, as discussed in [11], using the LMM can be found in a relevant publication [36]. In this method, the LMM steady cycle analysis procedure is utilised in tandem with a bisection convergence scheme in order to calculate the ratchet limit in an approximate manner. The fundamental premise of the LMM bisection procedure is to iteratively calculate the equivalent ratcheting strain for a given load cycle, then assess whether or not this is above or below a pre-defined target value of ratchet strain per cycle, before commencing a new calculation based upon a bisection of the calculated and target values of ratcheting strain. The main disadvantage of this LMM bisection method arises due to the search procedure which is implemented in order to achieve a convergent solution at the ratchet limit, which may be deemed inefficient and computationally expensive as a result,

especially for more complex and realistic models. The LMM bisection procedure also produces load multipliers which do not converge in the typical monotonic manner.

The main goal of this paper is to present the novel *generalised* LMM numerical procedure, which seeks to analyse the ratchet limit and associated failure mechanism with respect to thermo-mechanical load histories which vary proportionally and strictly in-phase throughout the defined load cycle, in a computationally *efficient* manner. The paper is subsequently structured as follows; initially an introduction to the cyclic continuum problem is presented in Section 2, followed by a brief description of the LMM steady-cycle analysis procedure in Section 3. Then the main Section 4 consisting of the proposed novel LMM ratchet analysis procedure is discussed. Two numerical comparisons are then conducted in order to verify the proposed methodology in Section 5, followed by a discussion and conclusions based upon these comparison results.

2. Definition of the arbitrary thermo-mechanical cyclic problem

The problem may be considered a continuum mechanics viewpoint if an EPP body is evaluated which is subjected to a general cyclic load condition. The body has a volume V in which a cyclic history of varying temperature $\theta(x,t)$ is applied alongside a cyclic history of varying surface tractions $P(x,t)$, which act upon a section of the body's surface S, defined here as S_T. The remaining portion of the surface S, denoted here as S_U, is constrained to have a zero displacement rate $\dot{u} = 0$. A typical cycle can be deemed to occur between $0 \leq t \leq \Delta t$.

If the applied cyclic load history is re-interpreted in terms of the cyclic temperature and surface forces as;

$$F(x,t) = \lambda\theta(x,t) + \lambda P(x,t) \tag{1}$$

where λ is the load parameter and $\theta(x,t)$ and $P(x,t)$ are reference cyclic histories of temperature and mechanical load respectively, varying with a typical cycle time equal to Δt. A linear elastic solution may be used to represent the thermal and mechanical loads from equation (1) in terms of stress;

$$\lambda\tilde{\sigma}_{ij}^{\Delta}(x,t) = \lambda\tilde{\sigma}_{ij}^{\theta}(x,t) + \lambda\tilde{\sigma}_{ij}^{P}(x,t) \tag{2}$$

With $\tilde{\sigma}_{ij}^{\Delta}(x,t)$ representing the elastic stress caused by the combined actions of the thermal stress $\tilde{\sigma}_{ij}^{\theta}(x,t)$ and mechanical stress $\tilde{\sigma}_{ij}^{P}(x,t)$ respectively. By assigning the load parameter λ to $\tilde{\sigma}_{ij}^{\Delta}(x,t)$, the potential to analyse an entire class of arbitrary loading paths is possible. The cyclic problem at hand involves the stress and strain histories being asymptotic to the cyclic state, where the Maximum Work Principle holds;

$$\tilde{\sigma}_{ij}(x,t) = \tilde{\sigma}_{ij}(x,t+\Delta t) \quad and \quad \dot{\varepsilon}_{ij}(x,t) = \dot{\varepsilon}_{ij}(x,t+\Delta t) \tag{3}$$

The total strain rate from equation (3) can be sub-divided into the individual elastic and plastic strain rates respectively;

$$\dot{\varepsilon}_{ij}^{e}(x,t) = \dot{\varepsilon}_{ij}^{e}(x,t+\Delta t) \tag{4a}$$

$$\dot{\varepsilon}_{ij}^{p}(x,t) = \dot{\varepsilon}_{ij}^{p}(x,t+\Delta t) \tag{4b}$$

This cyclic state will occur after an initial transient period [29]. The general cyclic problem is also assumed to incorporate a convex yield condition in order to define the plastic strains;

$$f(\sigma_{ij}) \leq 0 \tag{5}$$

as well as the use of an associated flow rule;

$$\dot{\varepsilon}_{ij}^{P} = \dot{\alpha}\frac{\partial f}{\partial \sigma_{ij}}\ ,\ f = 0 \tag{6}$$

where $\dot{\alpha}$ is the scalar plastic multiplier, thus the Maximum Work Principle may be stipulated as;

$$(\sigma_{ij}^{c} - \sigma_{ij}^{*})\dot{\varepsilon}_{ij}^{c} \geq 0 \tag{7}$$

With σ_{ij}^{c} is representative of the stress at yield $f\left(\sigma_{ij}^{c}\right) = 0$ and $\dot{\varepsilon}_{ij}^{c}$ is related to equation (6) in terms of the plastic strain rate $\dot{\varepsilon}_{ij}^{P}$. The term σ_{ij}^{*} depicts any allowable state of stress which satisfies the yield condition from equation (5).

The total stress solution relevant to the cyclic problem can be presented as;

$$\tilde{\sigma}_{ij}(x,t) = \lambda\tilde{\sigma}_{ij}^{\Delta}(x,t) + \rho_{ij}^{r}(x,t) \tag{8}$$

The problem may be construed as; the elastic solution $\tilde{\sigma}_{ij}^{\Delta}(x,t)$ (scaled by λ) and an accumulated residual stress history $\rho_{ij}^{r}(x,t)$ that represents the varying residual stresses within each cycle caused by any cyclic plasticity, which satisfies the condition;

$$\rho_{ij}^{r}(x,0) = \rho_{ij}^{r}(x,\Delta t) = \bar{\rho}_{ij}^{r}(x) \tag{9}$$

The constant residual stress $\bar{\rho}_{ij}^{r}(x)$ from equation (9) is a constituent component of the accumulated residual stress $\rho_{ij}^{r}(x,t)$ and can be seen to represent the state of residual stress at the beginning and end of each cycle. This term will be expanded upon further in Section 3, in the context of the numerical scheme.

The preceding discussion has mostly focussed on the cyclic stress histories, but the novel method which will be presented in this paper is fundamentally based on the strain rate histories associated with the ratcheting phenomena.

For non-ratcheting behaviour (where $\dot{\varepsilon}_{ij}^{p} \neq 0$) we have;

$$\Delta\varepsilon_{ij}^{p} = \int_{0}^{\Delta t} \dot{\varepsilon}_{ij}^{p}\, dt = 0 \tag{10}$$

However, for ratcheting behaviour, the varying plastic strain rate $\dot{\varepsilon}_{ij}^{p}$ is also non-zero but will invoke a net structural displacement mechanism per cycle. i.e;

$$\Delta\varepsilon_{ij}^{p} = \int_{0}^{\Delta t} \dot{\varepsilon}_{ij}^{p}\, dt \neq 0 \quad compatible\ with\ \Delta u_{ij}^{p} \neq 0 \tag{11}$$

It is worth noting that the relationship in equation (9) represents a closed loop of varying residual stress fields across all loading and unloading events within the load cycle, although this closed loop residual stress condition does not strictly preclude a net ratchet strain from occurring from one cycle to another (which is compatible with a net displacement Δu_{ij}^{p}); even though the cyclic stresses may have reached steady cyclic conditions.

This notion is also applicable to the asymptotic relationships in equations (3 & 4), i.e. ratcheting can still occur even when these stresses and strain rates exhibit a closed form solution from one cycle to the next.

3. Overview of the LMM direct steady cycle assessment (DSCA) procedure

The novel method that will be presented in Section 4 of this paper is based upon the steady-cycle analysis procedure of the LMM from [20], therefore a brief insight into this numerical scheme will be provided in this section to serve as a background for future discussion. The LMM steady-cycle analysis procedure may now be referred to as Direct Steady Cycle Analysis (DSCA) in the overall context of LMM framework.

In order to analyse a typical load cycle using the LMM, a series of elastic solutions are generated at various discrete time points within the cycle (for example at *n* locations in time, so that a subsequent series of elastic solutions is generated, $\tilde{\sigma}_{ij}^{\Delta}(x,t_n)$, where $n = 1,\dots N$ total number of load instances), such that the most significant stress ranges in the load cycle are encapsulated and hence the most significant plastic strains are used to correctly identify and calculate the ratchet mechanism caused by a given load cycle. It is postulated that the cyclic plastic strains will only occur at the load extremes stipulated by $n = 1,\dots N$.

By doing so, all other time points within the cycle are deemed innocuous in terms of significant plastic straining (due to the convexity of the yield surface) and are assumed to lie within the von Mises yield surface, thus allowing vast computational efficiency to be gained over cycle-by-cycle analysis (CCA) methods, which must analyse the entire load cycle and utilise a search procedure in order to obtain the ratchet limit itself.

The iterative DSCA procedure is concerned with the calculation of the accumulated residual stress history $\rho_{ij}^{r}(x,t)$ (from equation (8)) which is attributed to the history of varying plastic strains associated with the cyclic loads. The notation $\rho_{ij}^{r}(x,t)$ refers to the location in the volume (*x)* and point time during the cycle (*t)*, with the location (*x)* usually representative of an integration point in the FE mesh of the model.

By stipulating that the plastic strain increments may only occur at a predefined number of load extremes ($n = 1,\dots N$), we can sum the individual plastic strains $\Delta\varepsilon_{ij}^{n}$ which occur at each load extreme in order to obtain the ratcheting strain over the cycle $\Delta\varepsilon_{ij}^{R}$;

$$i.e. \quad \Delta\varepsilon_{ij}^{R} = \sum_{n=1}^{N} \Delta\varepsilon_{ij}^{n} \tag{12}$$

This is under the assumption that the loads follow a series of straight line paths in stress space and a strictly convex yield criterion is obeyed, i.e. all other load points in the cycle will be assumed to lie within the yield surface and hence rendered insignificant. The numerical DSCA methodology is based upon a series of iterative cycles which are defined as m = 1, 2... M. Within each iterative sub-cycle, there will be a series of increments *N*, i.e. for each load extreme ranging from $n = 1, \dots N$. Therefore, the primary emphasis of the LMM DSCA procedure is to iteratively calculate each individual varying residual stress $\Delta\rho_{ij}^{r}(x,t_n)_m$ associated with each elastic solution $\tilde{\sigma}_{ij}^{\Delta}(x,t_n)$, from $n = 1, \dots N$, until convergence is reached at cycle *M*. Upon reaching a converged solution, we can represent the constant residual stress term from equation (9) as;

$$\bar{\rho}_{ij}^{r}(x) = \sum_{m=1}^{M}\sum_{n=1}^{N}\Delta\rho_{ij}^{r}(x,t_n)_m \tag{13}$$

Thus, an equivalent expression for the accumulated residual stress $\rho_{ij}^{r}(x,t_n)$ at convergence can be seen in equation (14) as;

$$\rho_{ij}^{r}(x,t_n) = \bar{\rho}_{ij}^{r}(x) + \sum_{k=1}^{n}\Delta\rho_{ij}^{r}(x,t_k)_M \tag{14}$$

(Note that the definition of $\rho_{ij}^{r}(x,t_n)_m$ shown in Fig. 2 depicts the iterative and unconverged value of the accumulated residual stress history).

Convergence of the DSCA procedure can be adjudged using several criterions, but the variation in the matching modulus is most commonly used in order to define an acceptable level of convergence, i.e. when the change in modulus between iterative cycles reaches a specific target parameter. A flow-chart of LMM DSCA procedure has been highlighted in Fig. 2. A more comprehensive encapsulation of the iterative DSCA procedure is provided in [20].

4. Proposed novel LMM *generalised* procedure for ratcheting analysis of arbitrary cyclic thermo-mechanical loads

4.1 Background to proposed novel method

In the following sections of this paper the modified load regime consisting of cyclic thermal and mechanical loads which simultaneously vary in a proportional manner shall be referred to as *Type i)* loading and the classic Bree loading scenario of a cyclic thermal load range plus an additional constant mechanical load shall be referred to as *Type ii)* loading. It is worth noting that for Type ii) loading, the fixed cyclic load range can include thermal and mechanical loads respectively, but with the ratchet limit still being identified with respect to an additional constant (primary) loading. The generalised LMM presented in this paper is implemented using the UMAT and URDFIL subroutines in ABAQUS FE software [37].

As far as the Authors are aware there are no plasticity bounding theorems which are capable of *directly* assessing Type i) cyclic thermo-mechanical load histories. In order to overcome this hurdle, the LMM numerical procedure introduced in this paper has incorporated the DSCA procedure developed in [20] into a revised ratcheting analysis scheme in order to tackle the Type i) thermo-mechanical problem in a computationally efficient manner. This enables the calculation of ratchet limits with respect to proportional cyclic load variations to be conducted, with the ratchet limit being defined in terms of a predefined magnitude of maximum equivalent ratchet strain per cycle.

The novel LMM numerical scheme that is presented in this paper seeks to define the combined action of the cyclic thermal and mechanical loads via single load parameter. This logic is depicted in Fig. 3 where the scaling path of the previously mentioned two stage LMM ratchet analysis scheme from [20] (shown in red) and the proposed novel numerical method in this paper (shown in green) can be seen. Fig. 3 essentially represents a re-interpretation of the class of problem, by means of the relevant load-interaction schematic, for the modified Type i) loading regime compared to that of the original Type ii) Bree case. As is evident in Fig. 3 (from the analytical results of Bradford [11]), for Type i) loading compared to the Bree Type ii) loading, an augmented and noticeably more benign ratchet boundary is observed. It is also apparent from Fig. 3 that the strict shakedown limit (or reverse plasticity limit) varies from the existing Bree solution due to the variation in the cyclic stress range; as a result of considering a (cyclic) proportional load scaling path.

In order to calibrate the numerical method presented in this paper as well as to provide verification data, the analytical solutions of Bradford [11] for the Bree cylinder have been utilised. The second example involving the holed plate problem has been tested and verified using standard CCA techniques. The holed plate is useful for the purpose of illustrating the failure mechanism associated with a proportional loading regime, as the typical solution of the ratchet limit for an additional constant loading is well known, which serves to further emphasise the variation in the results presented later in this paper. Traditional CCA is used for verification purposes where needed, with EPP constitutive modelling being used as a standard.

4.2 The proposed novel numerical method

The novel method presented in this paper is herein referenced as the LMM *generalised* ratchet analysis procedure. This method utilises DSCA in order to assess the maximum ratchet strain across a structure, but instead of using a bisection convergence scheme [36], the load multiplier is reduced using an iterative scheme which decreases the rate of convergence relative to the applied loading and the iteratively scaled elastic stresses; which enables the decrement size between each iterative load multiplier to be reduced as the ratchet limit is approached.

The method commences by calculating the limit load due to the applied elastic stresses, $\tilde{\sigma}_{ij}^{\Delta}(x, t_n)$, which enables any applied reference load to be used, as well as ensuring a logical and efficient starting location for the analysis to ensure that a monotonic convergence scheme is observed. The limit load is calculated as a special case of the standard LMM shakedown procedure [38], which is modified so that only a single load instance forms the load cycle. The DSCA method as a stand-alone procedure can be used to obtain the steady cycle stresses and strain rates for a given combination of loading, similar to the application of DCA [12], but must be utilised with an appropriate convergence scheme in order to *directly* locate the ratchet limit in an efficient manner.

The novel convergence process of the generalised methodology is fundamentally based on setting a desired tolerance on the percentage difference between the load multipliers obtained from each iterative sub-cycle of the method; such that initial load multiplier (corresponding to the starting limit load starting point) eventually converges to load multipliers λ_i and λ_{i+1} which are within 1% of one another between sub-cycles. Where λ_i = previous sub-cycle multiplier and λ_{i+1} = updated multiplier. If a percentage error between consecutive load multipliers is set to a value *e* (e.g. 1%), this can be seen as;

$$\frac{\lambda_i - \lambda_{i+1}}{\lambda_i} \leq 1\% = e \tag{15}$$

Each sub-cycle involves calculating the maximum equivalent ratchet strain $\bar{\varepsilon}^R_{max}$ across the structure for a given set of elastic stresses $\tilde{\sigma}^{\Delta}_{ij}(x, t_n)$ scaled by a load multiplier λ_i. The quantity β is defined as;

$$\beta = \bar{\varepsilon}^R_{max} \cdot \frac{e\lambda_i}{\varepsilon^R_C} \tag{16}$$

Where ε^R_C is the target magnitude of equivalent ratchet strain per cycle and is used as the stopping criterion of the method; to define when the ratcheting mechanism is deemed to have been reached. The collective entities in the RHS of equation (16), which are used in order to reduce the previous iterative value of λ_i , can collectively be named as the decrement term β.

Therefore the relationship used to calculate a new load multiplier λ_{i+1} can be stipulated as;

$$\lambda_{i+1} = \lambda_i - \beta \tag{17}$$

The predefined value of ε^R_C is typically no less than 0.02%/cycle, due to numerical errors that can arise in the calculation of ratcheting strain using modern FE software.

In equation (17), it is apparent that as the calculated value of $\bar{\varepsilon}^R_{max}$ approaches the target value of ε^R_C, then the variation between consecutive load multipliers will reduce to 1% (i.e. $\lambda_{i+1} = \lambda_i - e\lambda_i$).This logic ensures that in the initial sub-cycles, where $\bar{\varepsilon}^R_{max}$ is relatively large (due to starting from the limit load), then the resulting decrement between the initial iterative load multipliers will also be comparatively large. As the load multipliers begin to monotonically reduce after several sub-cycles, the magnitude of $\bar{\varepsilon}^R_{max}$ calculated also reduces, which naturally means that the decrement between λ_{i+1} and λ_i will also reduce, ensuring a smooth convergence scheme as well as being computationally efficient. Equation (17) ensures the decrement size is dynamically changed based upon the iteratively scaled elastic stress fields and their relative value of $\bar{\varepsilon}^R_{max}$, as opposed to using a fixed decrement size which may be deemed computationally inefficient.

However, equation (17) alone is insufficient in ensuring that adequate decrements are observed between each consecutive sub-cycle and as such a restricting criterion has been

implemented on each value of $\bar{\varepsilon}^R_{max}$ obtained which ensures that the variation between λ_{i+1} and λ_i across each iterative sub-cycle is adequate, i.e.;

$$If \quad \bar{\varepsilon}^R_{max} > \frac{1}{K}.\frac{\varepsilon^R_C}{e} \tag{18}$$

$$Then \quad \bar{\varepsilon}^R_{max} = \frac{1}{K}.\frac{\varepsilon^R_C}{e} \tag{19}$$

Where *K* is a user defined value which stipulates the minimum number of sub-cycles that must be calculated from the initial load multiplier (at the limit load in the first sub-cycle) to the converged solution at the ratchet limit. Hence the quantity 1/*K* in equation (18) is in effect representative of the rate of convergence, e.g. *1/K = 1/10* (i.e. 1/minimum sub-cycles specified) = 0.1. As K is an important parameter with regards to convergence, the Authors recommend a default value of 10 be used as a minimum. The entity ε^R_C/e in equation (18) is fixed throughout the calculation. An overview of the LMM generalised ratchet analysis numerical procedure is summarised in Fig. 4, for an example initial cycle of the process.

The convergence controls shown through equations (17-19) do not strictly prohibit the load multiplier from crossing the target solution at the ratchet limit and hence a safeguard has been put in place in order to diminish this effect so that if this does occur then it becomes negligible. The safeguard process put in place involves assessing the magnitude of $\bar{\varepsilon}^R_{max}$ after each sub-cycle and if this value falls below the target magnitude ε^R_C after any sub-cycle, then the convergence criteria will be drastically reduced in order to minimise this effect, i.e. $\beta\ x\ 0.05$ from equation (17) and therefore the subsequent variation of λ_{i+1} in equation (17) between sub-cycles will become significantly smaller as a result. This process places further importance on the term *K* (which is specified *a priori)* and as such this value should be no smaller than 10 in order to ensure that if λ_{i+1} does fall below the actual ratchet load multiplier λ^R then the resulting effect will be negligible.

A further facet of the method includes the potential for considerable computational efficiency to be gained if the initial elastic reference loads (scaled along a proportional trajectory in the load domain) correspond to a ratchet limit which is coincidental with the limit load boundary, as can be seen in Fig. 3 for cyclic thermal loads below 1 on the normalised plot. In such an event, the first sub-cycle will produce a value of $\bar{\varepsilon}^R_{max}$ which is almost equal to ε^R_C (within a certain tolerance, e.g. $\bar{\varepsilon}^R_{max} \leq 5.\varepsilon^R_C$ in the first sub-cycle). If this situation arises in the first sub-cycle, the

convergence parameters e and K are altered such that $e=e/20$ (e.g. 1%/20), $K = K + 10$ and $\beta = \beta\ x\ 0.05$. By doing so, the subsequent reduction in the load multipliers according to equation (17) will significantly small, as the method will have effectively recognised that the ratchet and limit load are coincidental.

The main reason behind the logic in equations (15-19) is to provide a load multiplier reduction scheme that reflects the current state of strain at the end of each iterative sub-cycle in the form of a suitable ratio and target convergence tolerance. Equations (15-17) provide numerically efficiently reductions of the load multiplier in terms of the ratio of target ratchet strain *to* the quantity of ratchet strain calculated after each sub-cycle across the structure.

Various convergence criteria may be used to govern how many increments will occur during each sub-cycle of the method, however the variation of the linear matching modulus from one sub-cycle to the next (using volume integrals of the shear modulus, i.e. for each FE integration point across each load instance) is deemed as being most practical, within a certain pre-defined convergence tolerance.

Because the proposed numerical procedure commences the calculation from the limit load region and converges to the ratchet limit (for a particular loading path), the method can also post-process the maximum plastic and total strain ranges associated with each of the various scaled elastic stresses which are produced by each iterative load multiplier as λ converges to the ratchet limit. These strain ranges provide key information concerning fatigue crack initiation in low cycle fatigue.

5. Numerical examples

5.1 Bree cylinder

The Bree cylinder problem provides a simple uniaxial example of the method, as well as allowing for comparisons to be made with published analytical results for verification purposes [11]. The plane stress Bree cylinder case has been illustrated in Fig. 5 i), with the problem representative of the fuel clad in a fast reactor configuration [4]. A cyclic thermal load was applied to the inner surface of the cylinder, alongside a cyclic internal pressure. The applied cyclic load history is depicted in Fig. 5 ii), where both the thermal and mechanical loads can be seen to vary in-phase with one another, thus the problem may be characterised by two load extremes; *on-load* (σ_p and $\theta_0 + \Delta\theta$) and *off-load* (where both loads are simultaneously removed to a zero stress state). This loading history can also be characterised in a load domain plot, as

shown in Fig. 5 iii). The model was constrained vertically at one end and allowed to expand in-plane at the other, with a thrust applied to the free end to simulate the closed-end condition. The FE model is constructed using plane stress conditions in order to generate comparison results with Bradford [11]. Plane stress modelling conditions have been utilised in order to develop the novel numerical LMM presented in this paper; as for a von Mises yield condition the solution for plane stress equals the Tresca solution, thus ensuring the most conservative case of the Bree problem is modelled. The following temperature independent material properties were used in the analysis: thermal conductivity = 0.0215 W/mm°C, Young's Modulus = 184GPa, Poisson's ratio = 0.3, coefficient of thermal expansion = $1.84e^{-5}°C^{-1}$ and yield strength = 205 MPa.

In Fig. 6, the complete cyclic plasticity safety domain diagram for the modified Bree problem has been derived, using the LMM generalised procedure discussed in Section 4.2, which clearly depicts the relevant regions for each of the cyclic failure mechanisms. The analytical solution provided by Bradford [11] can be seen in Fig. 6 for comparison and verification purposes. In Fig. 6, two boundaries relative to the ASME III Code safety limits can also be seen; i.e. relative to the original and modified Bree problems respectively. The approximate ratchet limit found using the LMM generalised method (with respect to a ratchet strain per cycle equal to 0.02%) is also directly compared to the ratchet limit found using the bisection method from [36] in Fig. 6, where the abscissa represents the cyclic mechanical load and the ordinate displays the cyclic thermal load as normal, with both axes being *normalised* against the relative yield strength of the material. The ratchet limits obtained via the LMM generalised procedure and the LMM bisection method can be seen to vary marginally due to the convergence schemes used, i.e. a monotonic reduction scheme compared to a bisection search routine.

For this problem, 20 increments per load instance were used within each iterative sub-cycle (i.e. each sub-cycle contained 40 increments due to two load instances being modelled). In order to generate the full ratcheting boundary as seen in Fig. 6, several LMM calculations have been performed by using various load paths, with three distinct loading paths being used for the purpose of results post-processing, labelled as 'Load Case 1-3' in Table. 1. For each individual load path, the LMM generalised procedure begins by calculating the limit load boundary, in order to ensure an adequate starting point for the calculation as well as ensuring a monotonic reduction of the load multiplier.

Convergence characteristics of the load multiplier λ versus sub-cycle number can be seen in Fig. 7, which depicts the results of analysing the effects of altering the total amount of increments

per sub-cycle on the convergence of the method (relative to Load Case 3 in this instance), where L represents a *fixed* amount of increments per each load instance for the purpose of this convergence study (within each iterative sub-cycle of the method). Even though the load multiplier shows similar convergence characteristics for a range of total sub-cycle increment values in Fig. 7, the strain magnitudes and strain ranges obtained from the method are naturally more accurate as the total amount of increments per sub-cycle is increased. The analytical ratchet limit in Fig. 7 corresponds to the ratchet boundary provided by Bradford [11], denoted as λ^{RLIMIT}. The results in Fig. 7 illustrate that the novel method presented in this paper is not a lower or upper bound solution, with the total amount of increments used per sub-cycle being an important parameter relative to the accuracy of the results obtained.

In Fig. 8, the variation in maximum equivalent ratchet strain relative to the *normalised* load multiplier can be seen along a proportional scaling path between the ratchet limit and limit load boundary, with the load multiplier λ being normalised against the *final* converged multiplier at the ratchet limit λ^R for each load case for clarity. Fig. 8 shows a common trend as the load multiplier approaches the ratchet limit from the limit load boundary, with the limit load multiplier λ^L shown for illustration purposes. Naturally, the ranges of load multipliers shown in Fig. 8 are relative to the distance between the ratchet limit and collapse boundary for each of the 3 distinct loading paths used. In Fig. 8, all of the results can be seen to converge to the target 0.02% predefined ratcheting strain measure at a normalised loading equal to 1 (i.e. at the numerical ratchet limit).

Fig. 9 illustrates the variation of the maximum plastic strain and maximum total strain ranges relative to the normalised load multiplier (from the ratchet limit to the limit load boundary), with both strain ranges being based on an EPP model. In Figs. 8 & 9, as the load multipliers are normalised against the exact ratchet limit multiplier, values corresponding to approximately 1 on the x-axis represent the ratchet limit, with the plot lengths varying based upon how far the ratchet limit is from the limit load boundary for each particular load case. In Figs. 8 & 9, the limit load multiplier for each load case has also been highlighted.

5.2 Holed plate

The holed plate provides a basic 3D example in order to illustrate the applicability of the method beyond the simple uniaxial Bree case. This problem however is typically known for loading regimes similar to that of the Bree cylinder and as such results for proportional cyclic thermo-mechanical histories are not known by the Authors to currently exist in the existing

literature. Ratchet limits derived on the typical combined action of cyclic thermal loading plus an additional constant load will however provide a complimentary background to the novel modified limits presented in this paper. Hence this numerical benchmark example will use published results for the typical loading scenario from [20], in order to generate comparisons with the modified proportional regime of cyclic thermal loading plus cyclic mechanical loading. The problem consists of an applied temperature distribution $\Delta\theta$ at the edge of the hole radius, in tandem with a uniaxial tension P applied on opposite edges of the plate, as depicted in Fig. 10 i). The FE mesh used for the analysis is shown in Fig 10. ii). The holed plate has the same dimensions as used in [20], with the ratio between the diameter *D* of the hole and the length *L* of the plate equalling 0.2, with the ratio of the depth of the plate to the length *L* of the plate is 0.05.

The temperature-independent material data for the holed plate include; a yield stress $\sigma_y = 360MPa$, elastic modulus E = 208 GPa, Poisson's ratio $v = 0.3$ and a coefficient of thermal expansion equal to $5\ x\ 10^{-5}\ °C^{-1}$. A quarter model of the plate is used for the analysis due to symmetry conditions, with 20-node quadratic brick elements (ABAQUS C3D20R) used for the structural analysis. A thermal analysis is conducted with $\Delta\theta\ = 100°C$ at the inner bore of the hole, with the edge of the plate remaining at a constant $\theta_0\ = 0°C$ (using DC3D20). This temperature field is then scaled in order to have various cyclic temperature ranges for the generation of a Bree-like interaction diagram. The maximum thermo-elastic von Mises effective stress occurs at the edge of the hole, which is governed by the applied temperature difference $\Delta\theta$. Hence the extremes of the load history are characterised by σ_P and $\Delta\theta$, as depicted in Fig. 5 ii), i.e. the temperature around the edge of the hole $\bar{\theta}(t)$ varies between θ_0 and $\theta_0 + \Delta\theta$.

In Fig. 11, two approximate ratchet limits are shown for the holed plate problem, relative to a maximum equivalent ratchet strain tolerance equal to 0.04%, obtained using the LMM generalised procedure and the LMM bisection method from [36] for comparison.

The target tolerance for this problem has been increased to 0.04%/cycle due to the 3D nature of the problem. Similar to the Bree example, three individual loading paths have been used for the purpose of results post-processing, labelled as 'Load Case 1-3' in Table. 2. Details of the load multiplier convergence characteristics relative to each iterative sub-cycle for the holed plate problem can be seen in Fig. 12, for Load Case 1-3 respectively. Information regarding the maximum equivalent ratchet strain relative to the three loading paths used (Load Cases 1-3) can be seen in Fig. 13, as well as details of the maximum equivalent plastic & total strain ranges in Fig. 14. In Figs. 13 & 14 the load multipliers are normalised against the converged numerical

ratchet multiplier for each load case. In Figs. 13 & 14 it is evident that the ratcheting strain and maximum plastic/total strain ranges follow a similar trend relative to the level of loading; as the load multiplier increases the ratchet strain and strain ranges steadily rise together in a near proportional manner with the load multiplier, as the level of loading approaches the collapse limit.

Another note to consider from Fig. 14 includes observing that both of the strain ranges do not tend to zero as the converged point corresponds to the converged ratchet limit at $\lambda/\lambda^R = 1$ as each respective strain range will reach zero at the strict shakedown limit instead of the ratchet limit. In order to verify the ratchet limits provided by the LMM generalised procedure several individual CCA calculations were conducted, as indicated by the blue, yellow and red markers in Fig. 11. In Fig. 11, for the traditional case of a constant loading being applied to a cyclic thermal stress range, the blue CCA load case locations indicate global shakedown, with the yellow and red CCA load case locations illustrating ratcheting behaviour. Conversely for the modified proportional problem, the yellow and blue CCA markers depict global shakedown, whilst the red CCA markers still exhibit ratcheting. Details relating to the magnitudes of plastic strain from CCA load cases 1, 2, 3 and 4 (from Fig. 11) for 100 applied load cycles, using an elastic-perfectly plastic material model, can be seen in Fig. 15. These results illustrate that CCA load cases 1 & 3 exhibit global shakedown whilst CCA load cases 2 & 4 display ratcheting behaviour for the proportional problem. These CCA results verify the change in ratcheting mechanism associated with cyclic thermo-mechanical loads which vary strictly in-phase compared to the original premise of applying a constant loading to a cyclic stress range.

The ratcheting failure mechanism produced by the novel LMM presented in this paper and the contours of plastic strain range associated with reference Load Case 2 can be seen in Figs. 16 & 17 respectively, for two levels of loading; i) at the numerical ratchet limit and ii) a level of loading $\lambda = 1.67$ between the ratchet and collapse limit (i.e. λ times the cyclic thermal and mechanical components of Load Case 2).

6. Discussion

The basic uniaxial plane stress Bree model provides a useful example in displaying the relevant plasticity mechanisms but does not serve as a fully robust test of the proposed numerical method due to the uniaxial nature of the ratcheting mechanism. The holed plate provides a step up in complexity by introducing 3D modelling conditions, but with no analytical solutions available.

For this problem CCA is used to validate the results generated. The holed plate remains a useful example due to the adequate level of complexity of the problem and the ease of conducting verification by CCA calculations, as well as the relatively large amount of solutions published in the literature with respect to an additional constant loading; which further exacerbate the differences in the modified ratchet limits discussed in this paper.

The novel LMM generalised method presented in this paper utilises a dynamically varying convergence scheme, which involves large initial increments in the iterative load multipliers, which eventually reduce in size as the ratchet limit is approached. The generalised method can also take into account and utilise the fact that for the proportional ratchet limit, at certain load levels, the ratchet limit will coincide with the limit load. If the structural problem being analysed contains a cracked body, then naturally no strict shakedown limit will be present and hence the bisection method [36] is incapable of assessing such problems. The generalised method however commences the iterative calculation process from the limit point (with the option to also conduct an initial shakedown analysis if needed), which eliminates this concern.

By starting from the limit load, the efficiency of the generalised method is much improved and the convergence is guaranteed compared to methods which may begin from starting stresses which are well beyond the collapse load. For ratcheting problems which involve purely cyclic mechanical loads, the ratchet limit will intersect the y-axis at a particular location and the difference between the ratchet limit and limit load will often be relatively small, meaning the generalised method will be notably effective in such circumstances.

One of the most notable features of the results presented in this paper is the modified ratchet limits produced by the novel LMM. Details of such modified interaction diagrams have a small footprint in the relevant literature, especially with regards to relating these augmented limits to realistic structural assessments and the relative outcome for Code assessments. By generating a greater understanding of the failure mechanism associated with arbitrary thermo-mechanical load histories, more overall efficiency may be gained in modern nuclear components by raising the operational conditions and removing any inherent conservatism that may exist. Such conservatism can be seen in the modified ASME III shakedown safety envelope which is shown to be over restrictive for all combinations of load types; which is derived by considering the primary stress to also have a *range*.

An underpinning facet of the method presented in this paper involves the use of ratchet tolerant design, via a strain based assessment procedure. The use of such a phenomenon for the cyclic problem at hand allows for realistic structural assessments to be performed which respect to arbitrary cyclic thermo-mechanical loads. A relevant ratcheting criterion to compliment the ratchet tolerant design concept used in this paper stems from the JPVRC ratcheting check [39], which involves ensuring that the total equivalent ratchet strain at the end of each cycle displays a decreasing trend, whilst the maximum value of the equivalent ratchet strain after each cycle is less than 0.01%. Around 5 to 10 cycles is suggested in order to obtain this 0.01% magnitude for practical reasons and hence this is deemed to show that the structure is shaking down to either elastic action or closed loop plastic cycling [39, 40].

7. Conclusions

A novel ratchet analysis procedure for evaluating proportional thermo-mechanical cyclic load histories has been presented, tested and verified in this paper using the LMM framework. The method presented in this paper has been used to overcome the difficulties associated with the LMM and the extended version of Koiter's upper bound for ratchet analysis, thus providing an insight into the consequences of altering the cyclic thermo-mechanical loads and the subsequent effect on the ratcheting failure mechanism relative to the ASME III Code. In order to assess the applicability of the method, two simple benchmark cases have been used to illustrate the numerical procedure in the Bree cylinder and holed plate problems. Detailed discussion has been provided in order to emphasise the feasibility of using such a ratchet tolerant design procedure for generating complete cyclic plasticity failure diagrams as well as unique verification analysis cases; where traditional cycle by cycle procedures can have difficulty in clarifying the actual failure response for 3D structural problems. The most apparent feature from the results presented in this paper is the modified ratchet limits produced from consideration of arbitrary thermo-mechanical load cyclic load histories. The effects of such phenomenon have herein been alluded to with respect to typical nuclear Code assessments for ratcheting and shakedown.

Acknowledgements

The authors gratefully acknowledge the Nuclear EngD centre of the United Kingdom, Michael Martin and Rolls-Royce Power Engineering plc. and the University of Strathclyde for their support during this work.

References

[1] ASME Boiler and Pressure Vessel Code, Section III, Rules for construction of nuclear power plant components, Div. 1, Subsection NB, class 1 components, 2007.

[2] ASME Boiler and Pressure Vessel Code, Section III, Rules for construction of nuclear power plant components, Div. 1, Subsection NH, Class 1 components in elevated temperature service, 2004.

[3] Miller, D.R, Thermal-stress ratchet mechanism in pressure vessels, Journal of Basic Engineering, Transactions of ASME, pp.190-196, 1959.

[4] Bree J, Elasto-plastic behaviour of thin tubes subjected to internal pressure and intermittent heat fluxes with application to fast reactor fuel elements. Journal Strain Analysis, pp.226-238, 1967.

[5] Ng, H. W., Moreton, D. N., Engineering approaches to high temperature design, Chapter 6, Bree diagrams for alternative loading sequences, (edited by Wilshire and Owen), 1983.

[6] Ng, H. W., Moreton, D. N., Ratchetting rates for a Bree cylinder subjected to in-phase and out-of-phase loading. J Strain Analysis Eng Des, 21;1, 1986.

[7] Ng, H. W., Moreton, D. N., Alternating plasticity at the surfaces of a Bree cylinder subjected to in-phase and out-of-phase loading. J Strain Analysis Eng Des, 22;107, 1987.

[8] Reinhardt, W., Distinguishing ratcheting and shakedown conditions in pressure vessels, PVP2003-1885, ASME PVP Conference, Cleveland, Ohio, USA, 2003.

[9] Abdel Karim, M., Shakedown of complex structures according to various hardening rules, International Journal of Pressure Vessels and Piping, vol. 82, pp 427-458, 2005.

[10] Staat, M., Heitzer, M., LISA - A European project for FEM-based limit and shakedown analysis. Nuclear Engineering and Design, 206, pp.151–166, 2001.

[11] Bradford, R. A. W., The Bree problem with primary load cycling in-phase with the secondary load, International Journal of Pressure Vessels and Piping, vol. 99–100, pp.44–50, 2012.

[12] Nguyen-Tajan et al, Determination of the stabilized response of a structure undergoing cyclic thermal-mechanical loads by a direct cyclic method. ABAQUS Users' Conference Proceedings, 2003.

[13] Martin, M. Application of direct cyclic analysis to the prediction of plastic shakedown of nuclear power plant components. Pressure Vessels and Piping, Chicago, Illinois, 2008.

[14] M. Martin, L. Rawson, D. Rice, A Hierarchical Finite Element Framework for the Assessment of Pressure Vessels to the ASME III Code, ASME Pressure Vessels and Piping Conference: Volume 1, pp. 125–135, 2010.

[15] Ponter, A.R.S, Carter, K.F., Limit state solutions, based upon linear solutions with a spatially varying elastic modulus, Comput. Methods Appl. Mech. Engrg. 140, pp.237-258, 1997.
[16] Ponter, A.R.S, Carter, K.F., Shakedown state simulation techniques based on linear elastic solutions, Comput. Methods Appl. Mech. Engrg. 140; pp.259-279, 1997.
[17] Ponter A. R. S, Chen H. F, A minimum theorem for cyclic loading in excess of shakedown, with applications to the evaluation of a ratchet limit, European Journal of Mechanics A/Solids, 20 (4) pp. 539-554, 2001.
[18] Chen H. F, Ponter A. R. S, A method for the evaluation of a ratchet limit and the amplitude of plastic strain for bodies subjected to cyclic loading, European Journal of Mechanics A/Solids, 20 (4), pp. 555-572, 2001.
[19] Chen, H., Ponter, A.R.S, Linear matching method on the evaluation of plastic and creep behaviours for bodies subjected to cyclic thermal and mechanical loading, Int. J. Numer. Meth. Engng, 68: pp. 13-32, 2006.
[20] Chen, H.F., Ponter, A.R.S., A direct method on the evaluation of ratchet limit, Journal of Pressure Vessel Technology, 132(4), 2010.
[21] Adibi-Asl, R., Reinhardt, W., Non-cyclic shakedown/ratcheting boundary determination – Part 1: Analytical approach, International Journal of Pressure Vessels and Piping, vol. 88, no. 8–9, pp. 311–320, 2011.
[22] Adisi-Asl, R., Reinhardt, W., Non-cyclic shakedown/ratcheting boundary determination. Part 2: Numerical implementation, Int. J. Press. Vess. Piping 88, pp. 321–329, 2011.
[23] Martin, M., Rice, D., A Hybrid Procedure for Ratchet Boundary Prediction, ASME Pressure Vessels and Piping Conference Volume 1: Codes and Standards, pp. 81–88, 2009.
[24] Spiliopoulos, K.V., Panagiotou, K.D., A direct method to predict cyclic steady states of elastoplastic structures, Comp. Methods Appl. Mech. Engrg. 223-224, pp. 186-198, 2012.
[25] Spiliopoulos, K.V., Panagiotou, K.D., A residual stress decomposition method for the shakedown analysis of structures. Comp. Methods Appl. Mech. Engrg. 276, pp. 410-430, 2014.
[26] Jappy, A., Mackenzie, D., Chen, H., A Fully Implicit, Lower Bound, Multi-Axial Solution Strategy for Direct Ratchet Boundary Evaluation: Theoretical Development, J. Pressure Vessel Technol, 135(5), 2013.
[27] Jappy, A., Mackenzie, D., Chen, H., A Fully Implicit, Lower Bound, Multi-Axial Solution Strategy for Direct Ratchet Boundary Evaluation: Implementation and Comparison, J. Pressure Vessel Technol, 136(1), 2013.
[28] Abou-Hanna, J., McGreevy, T.E., A simplified ratcheting limit method based on limit analysis using modified yield surface, Int. J. Press. Vess. Piping 88, pp. 11–18, 2011.

[29] Gokhfeld, D. A., Cherniavsky, O.F., Limit Analysis of Structures at Thermal Cycling, Suthoff & Nordhoff, Alphen aan den Rijn, The Netherlands, 1980.
[30] Muscat, M., Hamilton, R., Boyle J.T., Shakedown analysis for complex loading using superposition. J. Strain analysis, 37 (5), pp. 399-412, 2002.
[31] Muscat, M., Mackenzie, D., Hamilton, R., 2003 Evaluating shakedown under proportional loading by non-linear static analysis. Computers and Structures, 81 (17), pp. 1727-1737
[32] Abdalla, H.F., Megahed, M.M., Younan, M.Y.A., 2007. A simplified technique for shakedown limit load determination. Nuclear Engineering and Design 237, pp. 1231-1240.
[33] Abdalla, H.F., Megahed, M.M., Younan, M.Y., 2009, Comparison of pipe bend ratchetting/ shakedown test results with the shakedown boundary determined via a simplified technique, In: Proceedings of the ASME – PVP Division Conference, Prague, Czech Republic.
[34] Koiter W. T. General theorems for elastic plastic solids. Progress in solid mechanics J.N. Sneddon and R. Hill, eds. North Holland, Amsterdam, 1; pp. 167-221.,1960.
[35] Chen H.F., Ure J., Tipping D., Calculation of a lower bound ratchet limit part 1 – Theory, numerical implementation and verification, European Journal of Mechanics - A/Solids, 37, pp. pp. 361-368 , 2013.
[36] Lytwyn, M., Chen, H.F., Martin, M., Ratchet analysis of structures under a generalised cyclic load history, ASME PVP Conference, PVP2014-28326, Anaheim, California, USA, 2014.
[37] ABAQUS, Dassault Systemes, Version 6.11, 2011.
[38] Chen H.F., Ponter A.R.S., The 3-D shakedown and limit analysis using the linear matching method, International Journal of Pressure Vessel and Piping, 78, 443-451, 2002.
[39] Okamoto, A., Nishiguchi, I., and Aoki, M., New secondary stress evaluation criteria suitable for finite element analyses, ICPVT-9, Sydney, Vol. 2, pp. 613-620, 2000.
[40] Kalnins, A. Shakedown and ratcheting directives of ASME BP&V code and their execution. 439, ASME PVP Conference, Vancouver, Canada, pp. 47-55, 2002.

Table. 1 – Reference elastic load paths used for the Bree example.

Load Case	$\Delta\boldsymbol{\theta/100}$ $(°\boldsymbol{C})$	$\Delta\boldsymbol{\sigma_P}$ $(\boldsymbol{MPa})$
1	$0 \leftrightarrow 2.4$	$0 \leftrightarrow 0.945\ \sigma_Y$
2	$0 \leftrightarrow 4.2$	$0 \leftrightarrow 0.83\ \sigma_Y$
3	$0 \leftrightarrow 4.5$	$0 \leftrightarrow 0.62\ \sigma_Y$

Table. 2 – Reference elastic load paths used for the holed plate problem.

Load Case	$\Delta\boldsymbol{\theta/100}$ $(°\boldsymbol{C})$	$\Delta\boldsymbol{\sigma_P}$ $(\boldsymbol{MPa})$
1	$0 \leftrightarrow 3.0$	$0 \leftrightarrow 0.65\ \sigma_Y$
2	$0 \leftrightarrow 2.5$	$0 \leftrightarrow 0.4\ \sigma_Y$
3	$0 \leftrightarrow 4.0$	$0 \leftrightarrow 0.33\ \sigma_Y$

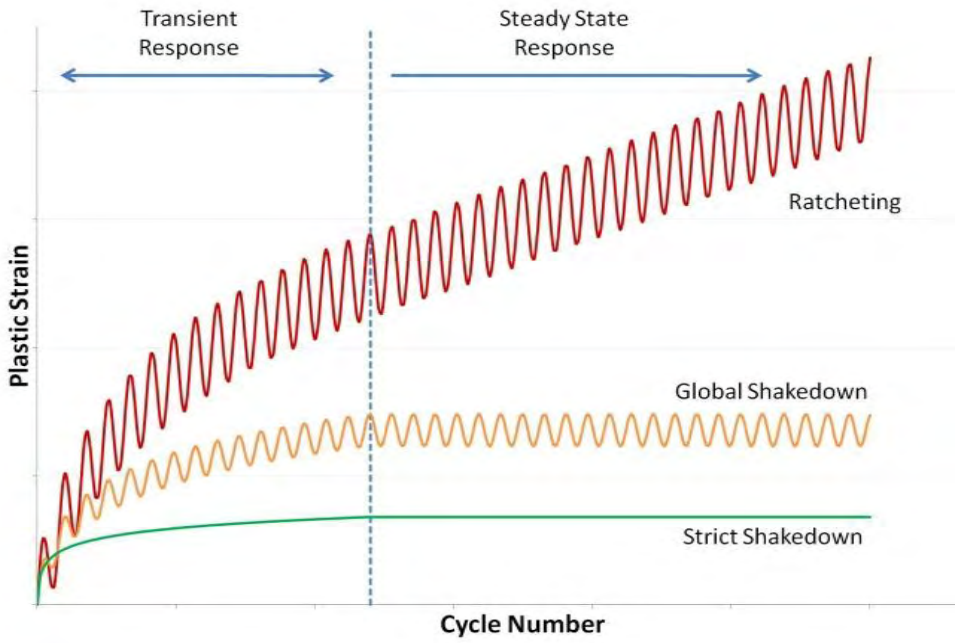

Fig. 1 - Typical plastic strain evolution behaviour for strict shakedown, global shakedown and ratcheting.

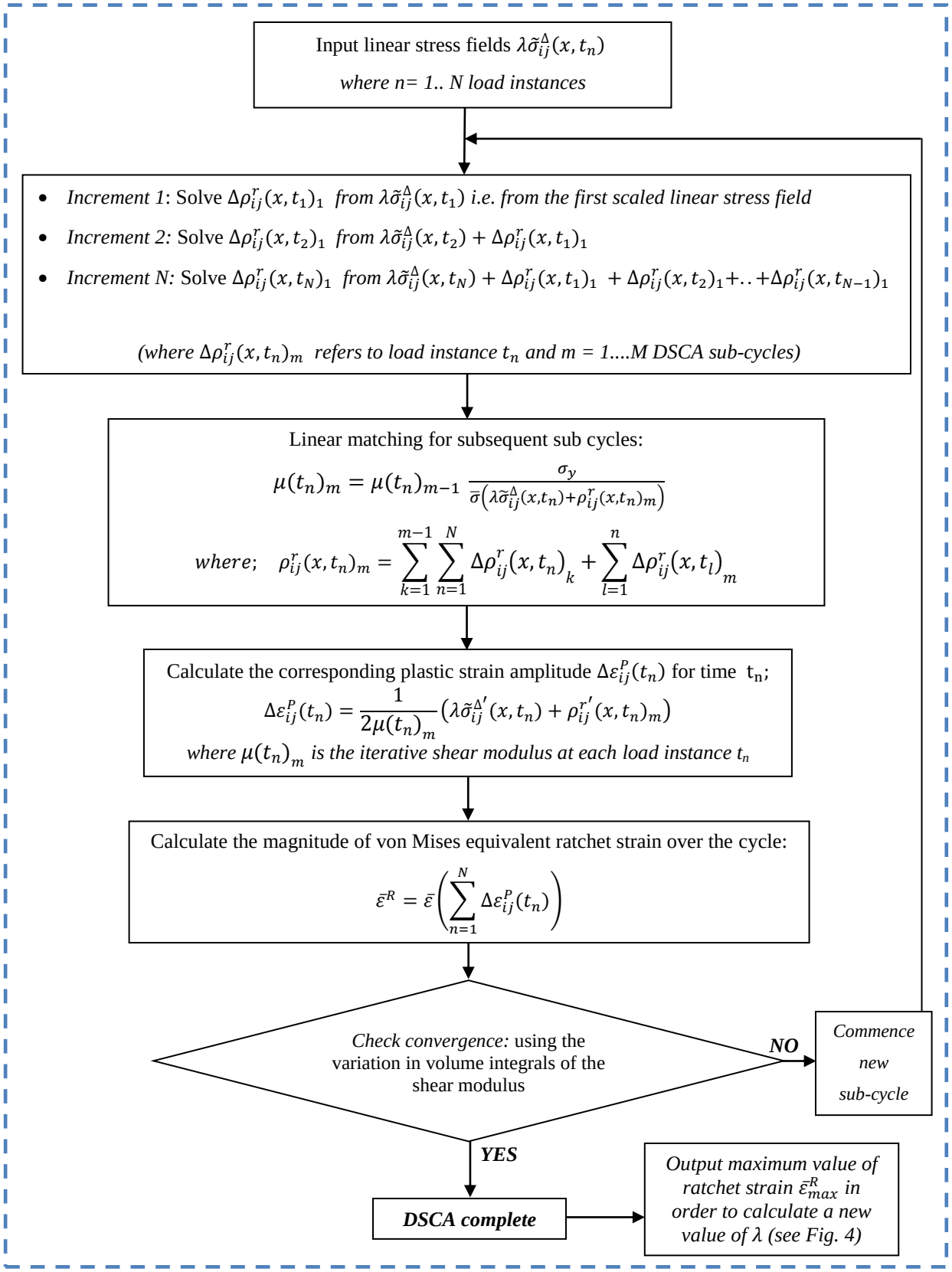

Fig. 2 - Flow chart illustration of the LMM DSCA numerical procedure.

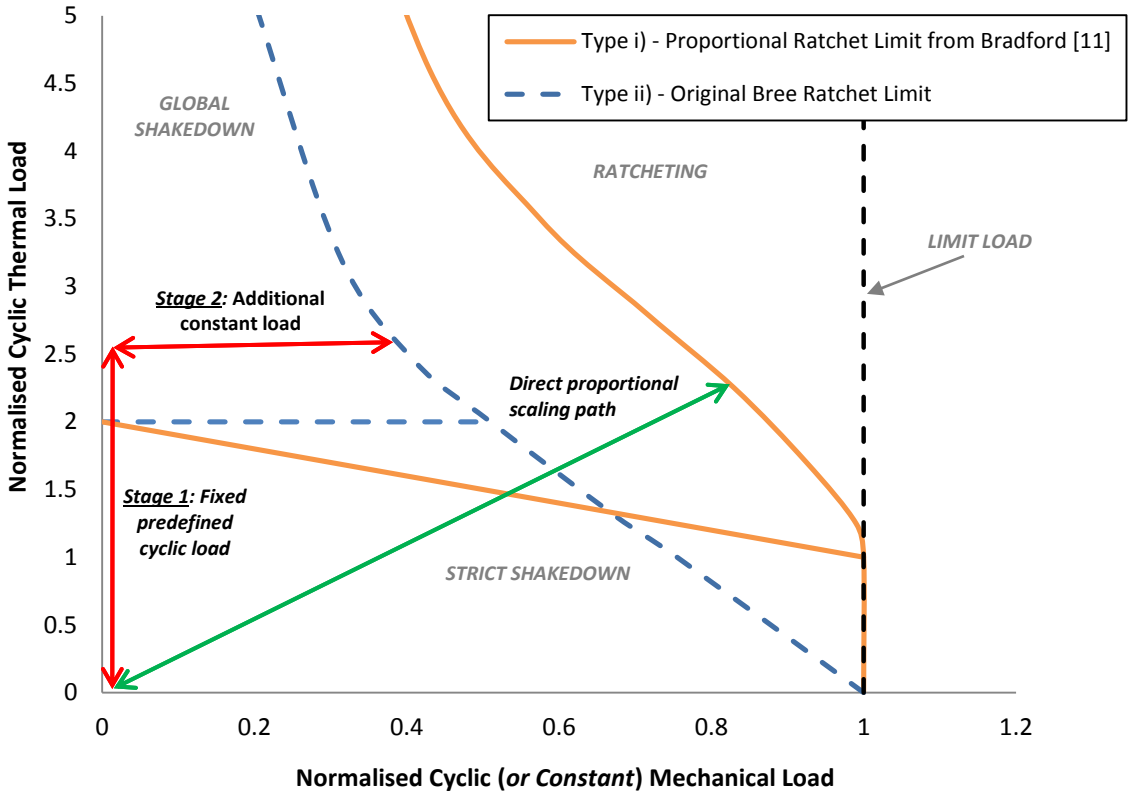

Fig. 3 - Load interaction diagram illustrating each failure regime for the classic Bree (Type ii) & modified problem (Type i)), as well as the LMM numerical load scaling paths.

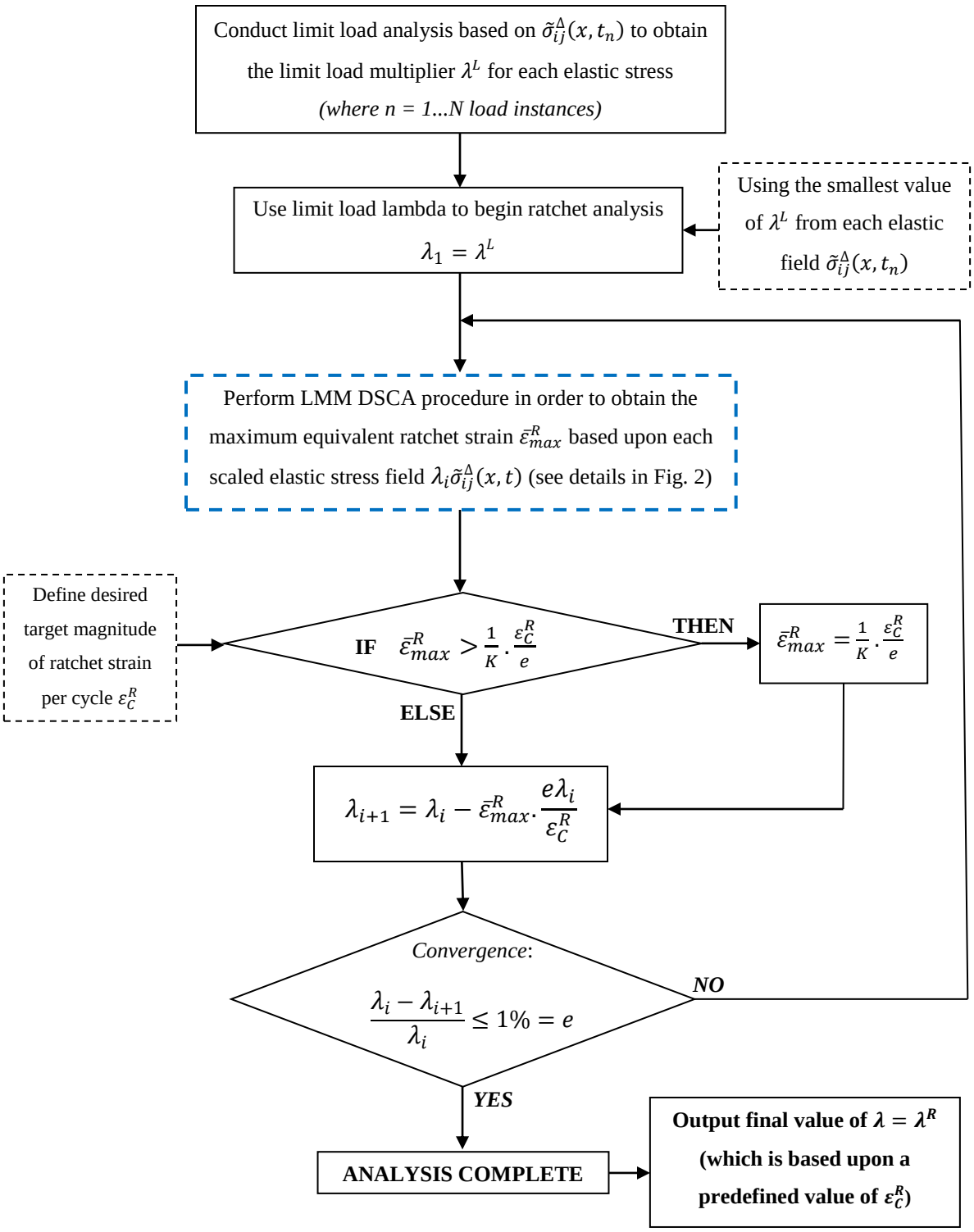

Fig. 4 - Flow chart of the novel LMM generalised ratchet analysis procedure (using e = 1%).

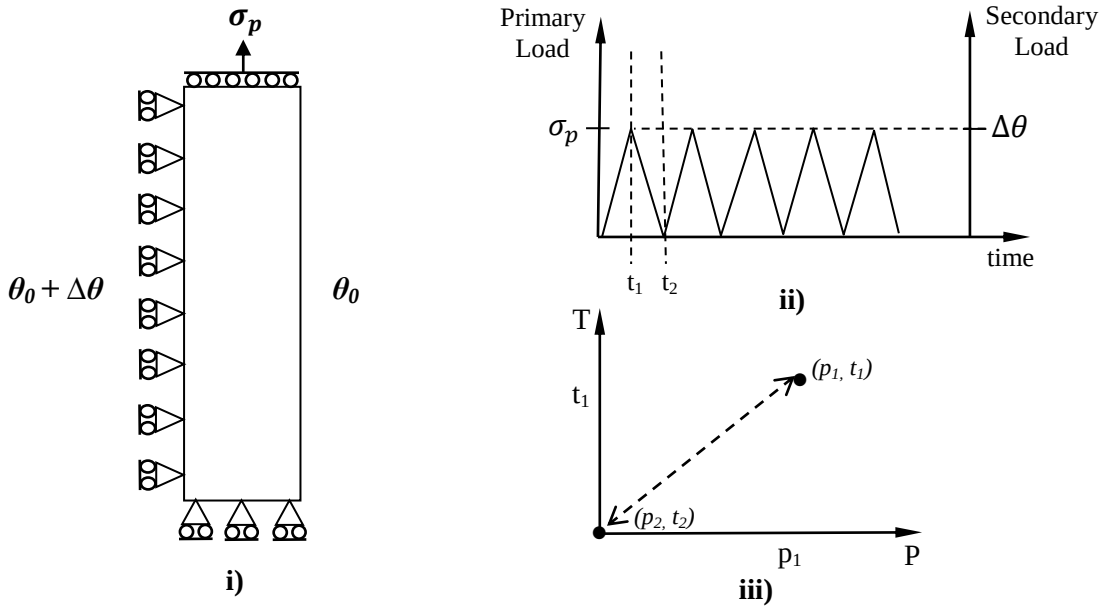

Fig. 5 i) Plane stress Bree model ii) applied cyclic thermo-mechanical load history and iii) in load domain.

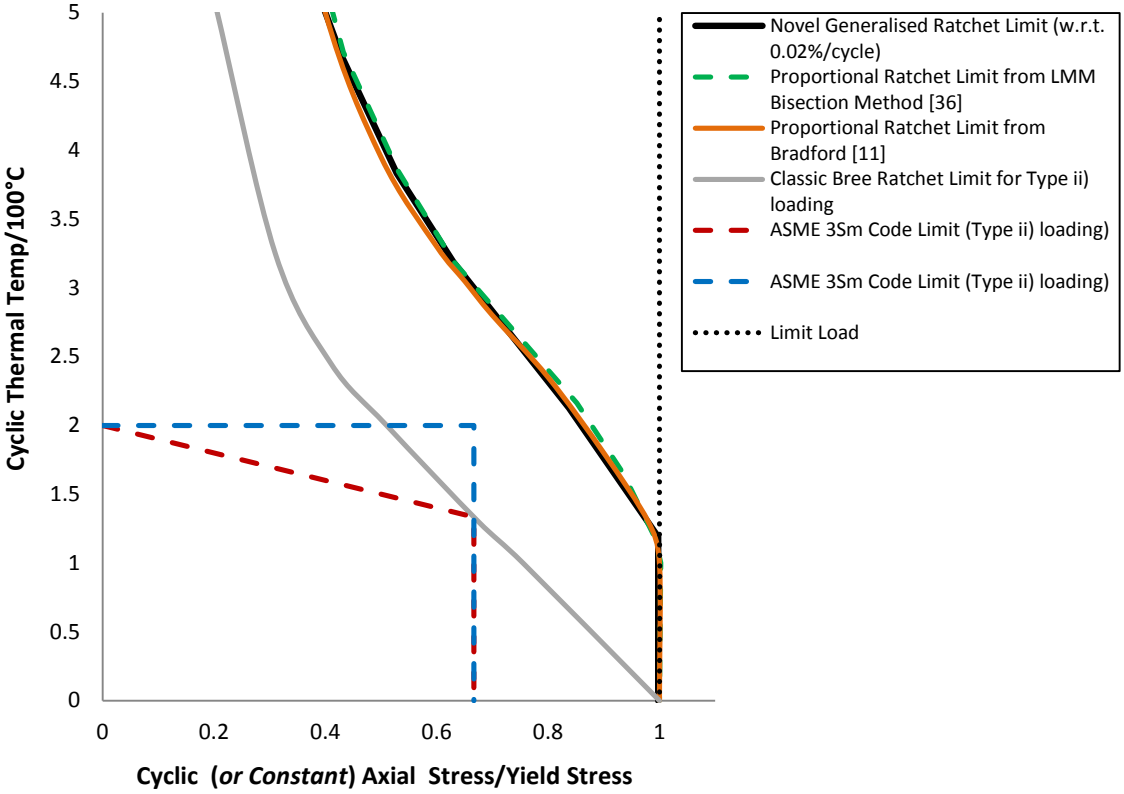

Fig. 6 - Bree problem ratchet boundaries for proportional loading compared to analytical solution of Bradford [11], alongside original Bree limit for constant loading and the relevant ASME III Code 3Sm limits for each respective loading regime.

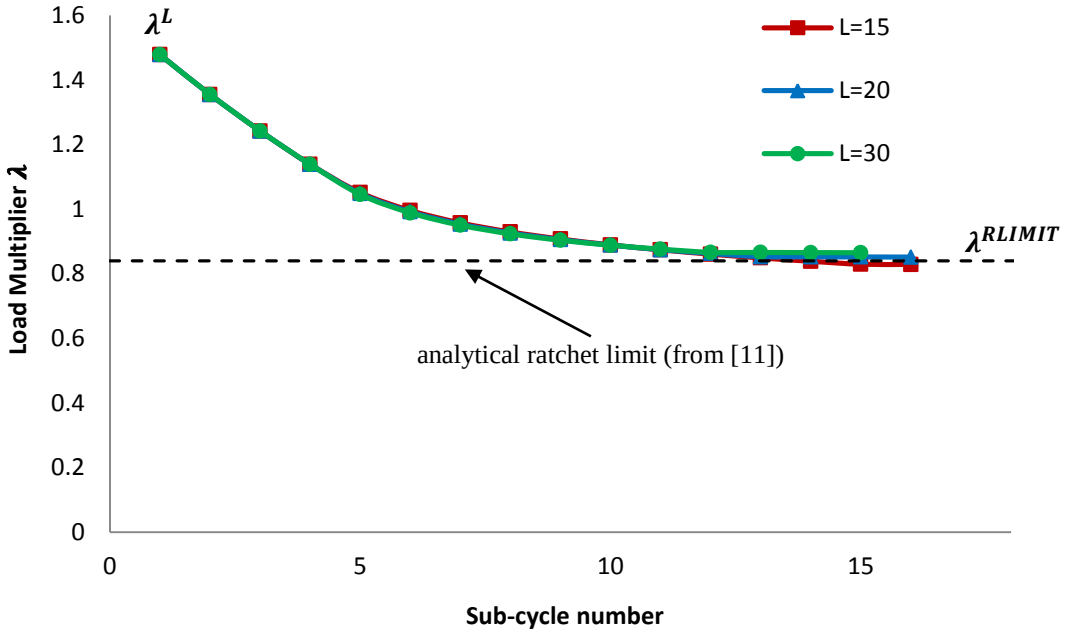

Fig. 7 – Generalised LMM load multiplier convergence characteristics for various amounts of *fixed* increments per sub-cycle (relative to reference Load Case 3).

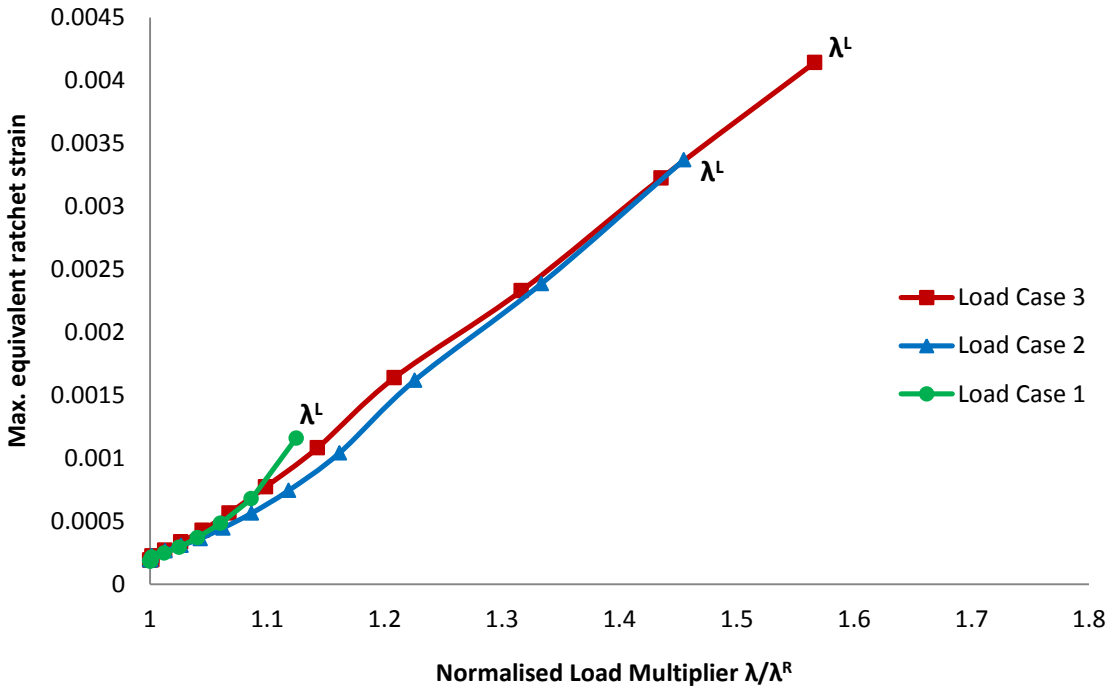

Fig. 8 – Maximum equivalent ratchet strain *vs*. *normalised* load multiplier.

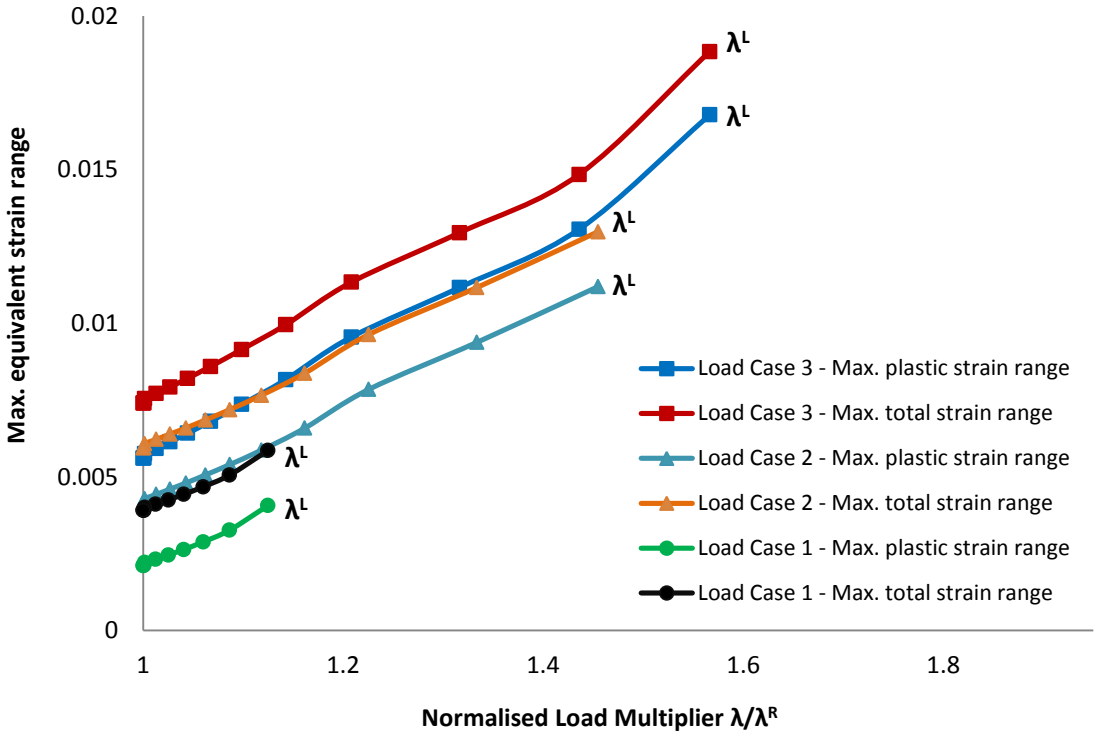

Fig. 9 – Maximum equivalent (plastic/total) strain ranges *vs*. *normalised* load multiplier.

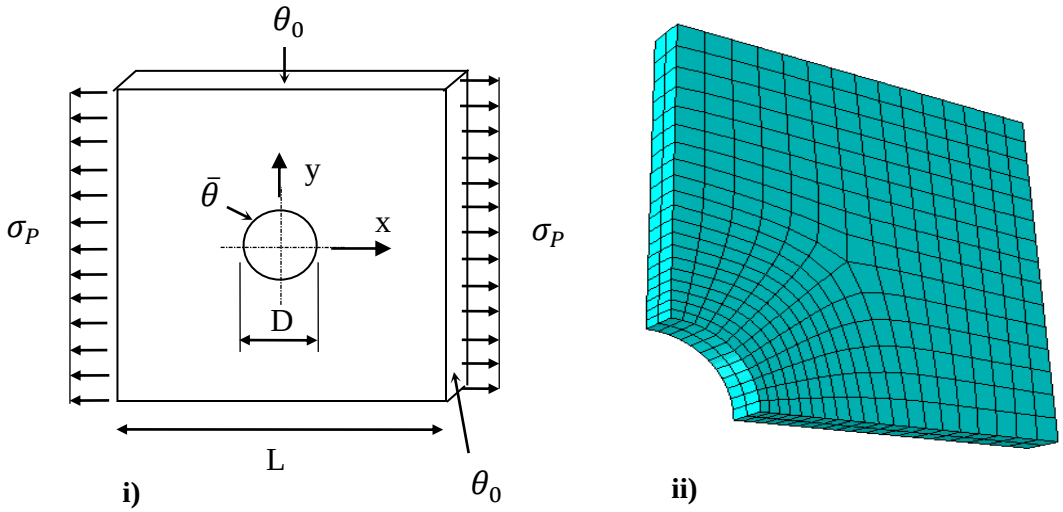

Fig. 10 - i) Holed plate problem geometry and ii) Quarter model FE mesh.

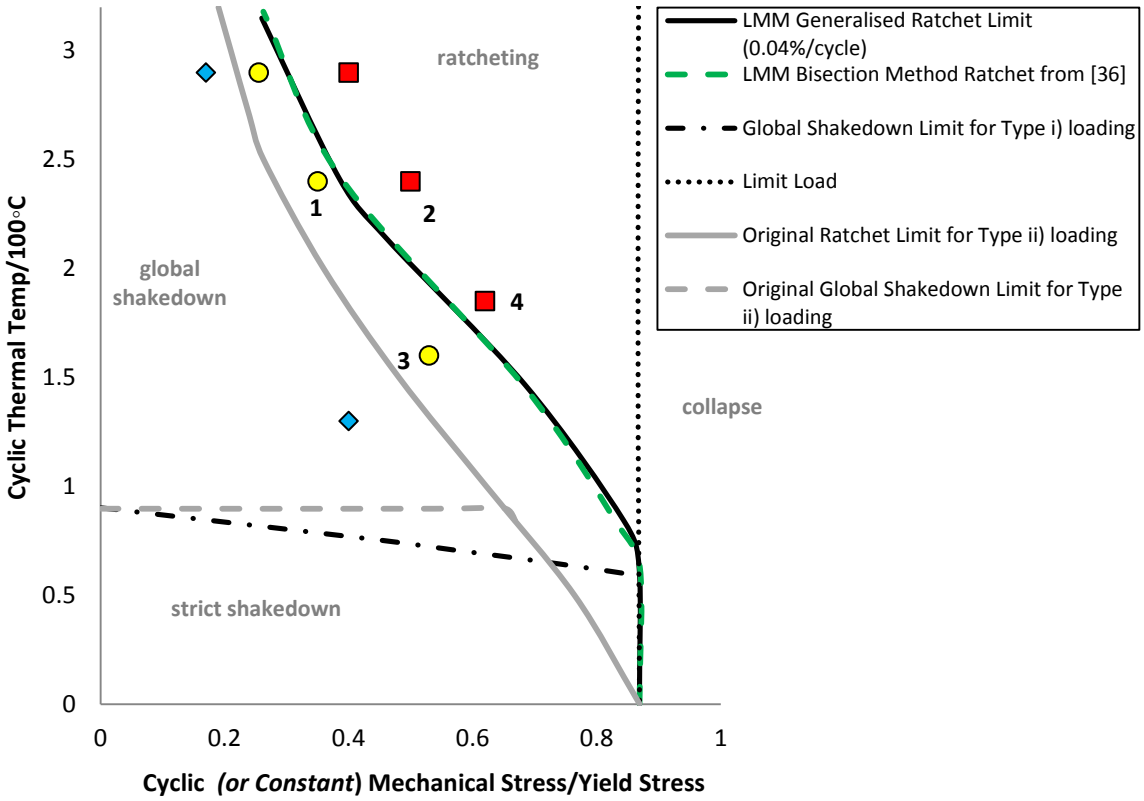

Fig. 11 - Holed plate ratchet boundaries for proportional loading and original Bree type loading (including locations for individual CCA load case calculations used to verify ratchet limit)**.**

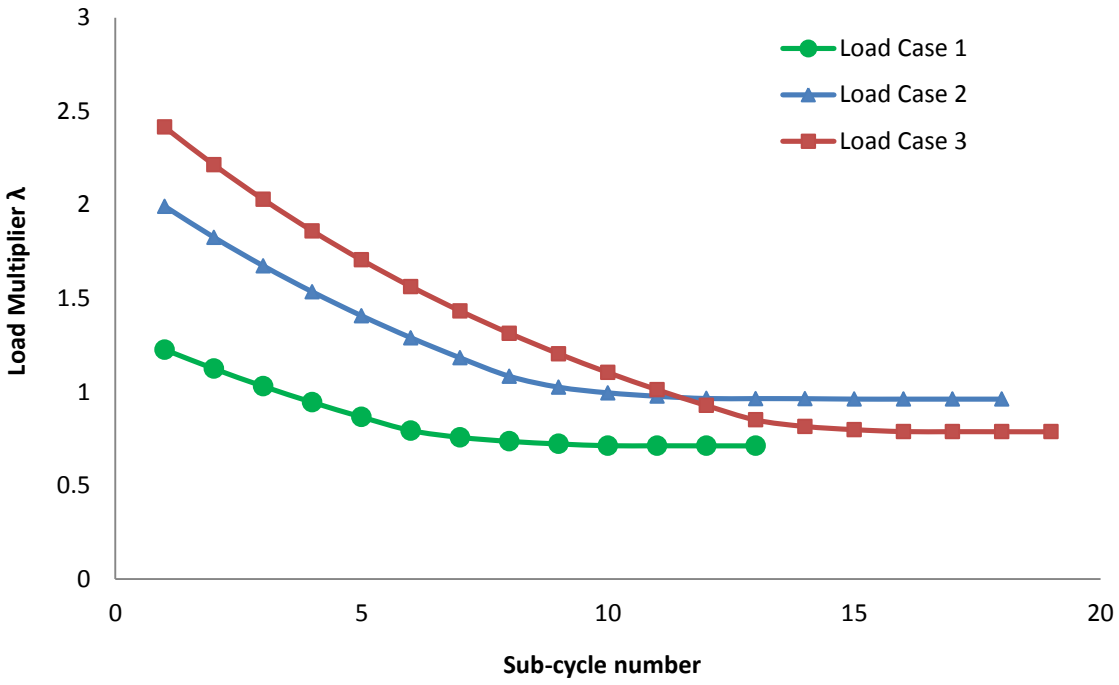

Fig. 12 – Load multiplier convergence characteristics for the holed plate problem.

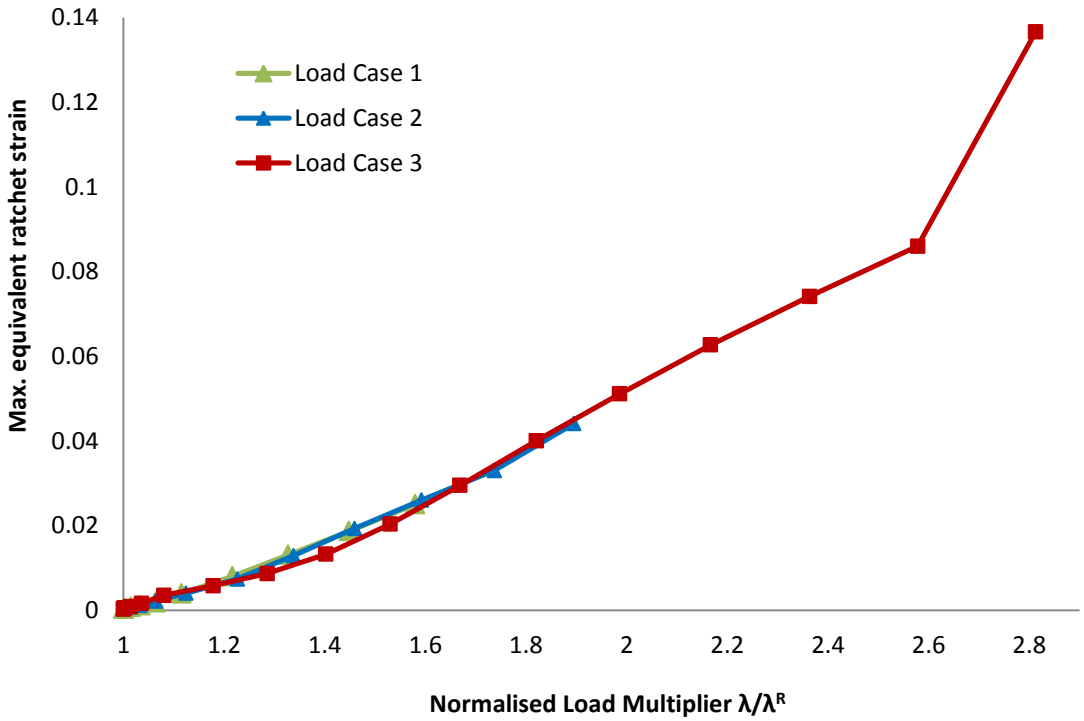

Fig. 13 – Maximum equivalent ratchet strain *vs*. *normalised* load multiplier for the holed plate.

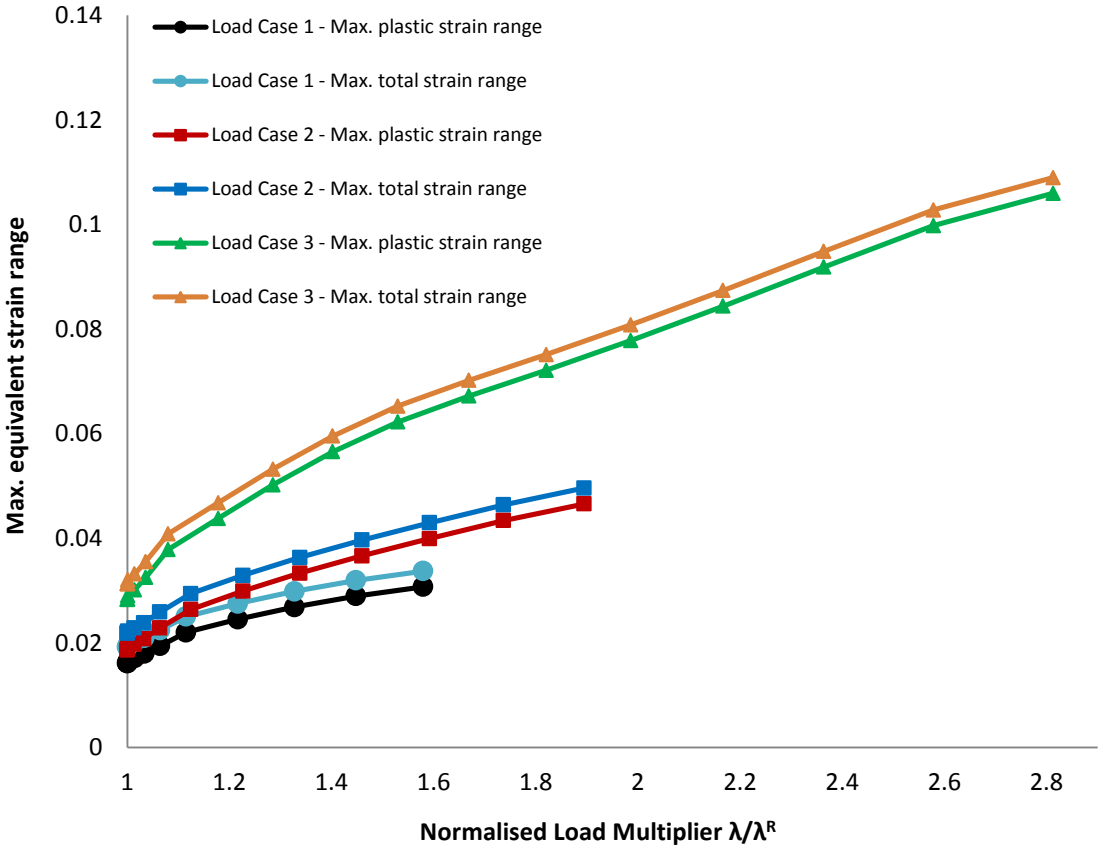

Fig. 14 – Maximum equivalent (plastic/total) strain ranges *vs*. *normalised* load multiplier.

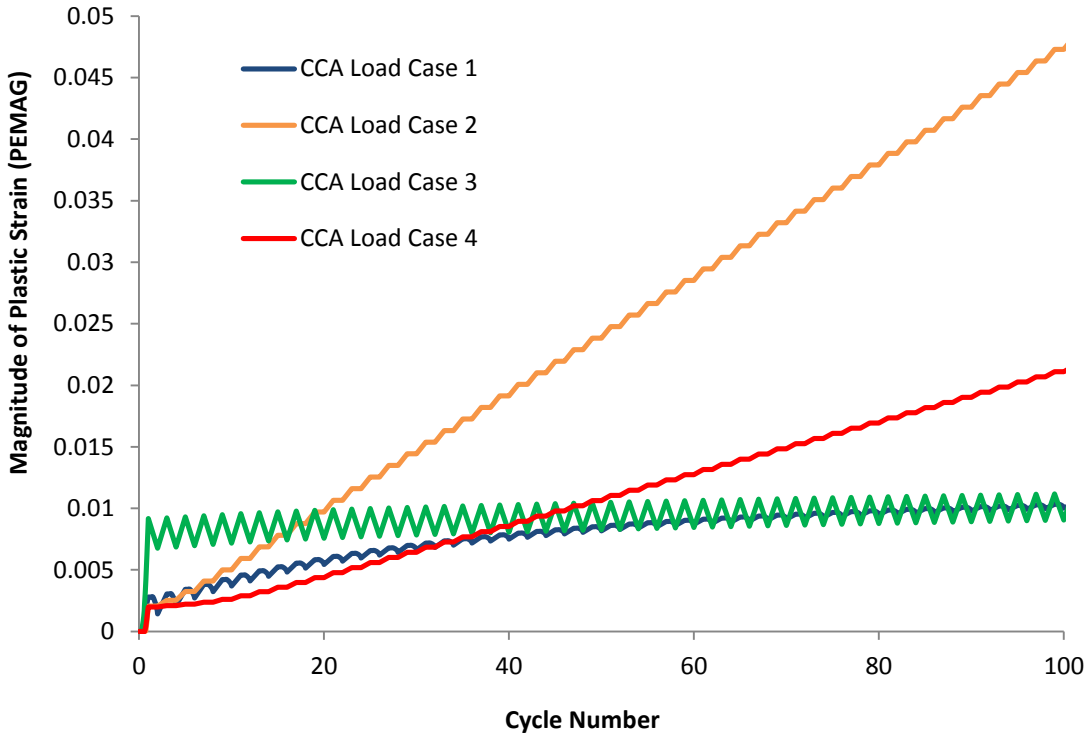

Fig. 15 - Magnitude of plastic strain results from sample CCA load cases 1, 2, 3 & 4 (from Fig. 11) of the holed plate ratchet boundary, illustrating ratcheting at points 2 & 4 and strict shakedown at 1 & 3.

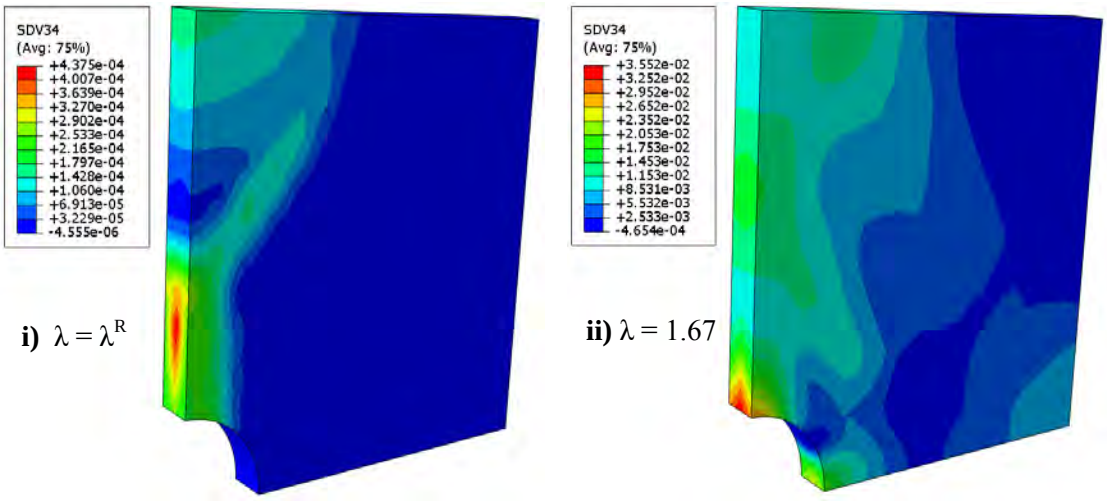

Fig. 16 – Contours of equivalent ratchet strain at various levels of loading; at i) $\lambda = \lambda^R$ and ii) $\lambda = 1.67$.

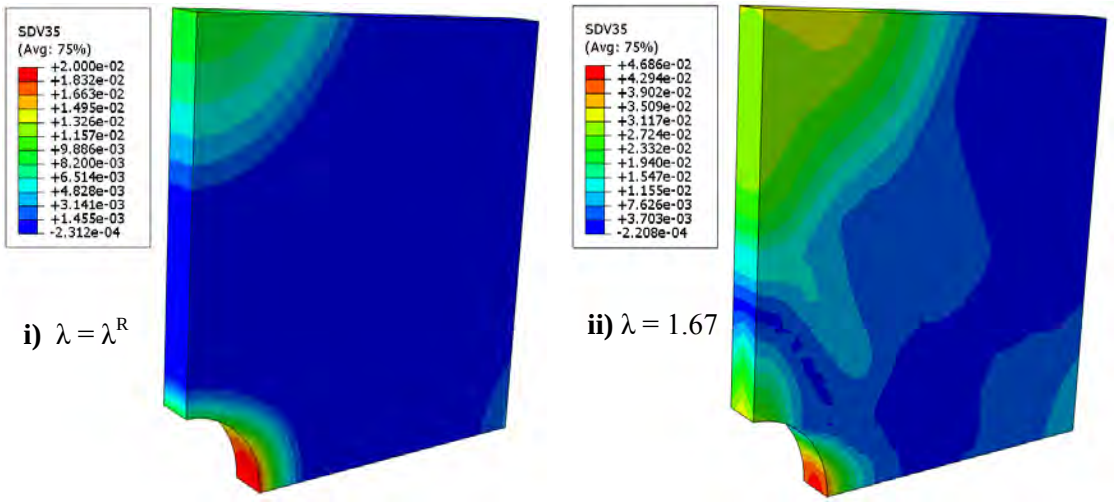

Fig. 17 - Contours of the equivalent plastic strain range at various levels of loading; at i) $\lambda = \lambda^R$ and ii) $\lambda = 1.67$.